PHILOSOPHICAL TRANSACTIONS B

rstb.royalsocietypublishing.org

Research

Cite this article: Taylor SH, Long SP. 2017 Slow induction of photosynthesis on shade to sun transitions in wheat may cost at least 21% of productivity. *Phil. Trans. R. Soc. B* **372**: 20160543.
http://dx.doi.org/10.1098/rstb.2016.0543

Accepted: 2 April 2017

One contribution of 16 to a discussion meeting issue 'Enhancing photosynthesis in crop plants: targets for improvement'.

Subject Areas:
plant science, physiology, computational biology, environmental science, biochemistry

Keywords:
food security, Rubisco, Rubisco activase, photosynthetic induction, wheat, crop yield improvement

Author for correspondence:
Stephen P. Long
e-mail: slong@illinois.edu

Electronic supplementary material is available online at https://dx.doi.org/10.6084/m9.figshare.c.3820807.

THE ROYAL SOCIETY PUBLISHING

Slow induction of photosynthesis on shade to sun transitions in wheat may cost at least 21% of productivity

Samuel H. Taylor[1] and Stephen P. Long[1,2,3]

[1]Lancaster Environment Centre, Lancaster University, Lancaster, Lancashire LA1 4YQ, UK
[2]Department of Crop Sciences, and [3]Department of Plant Biology, University of Illinois, Urbana, IL 61801, USA

SHT, 0000-0001-9714-0656; SPL, 0000-0002-8501-7164

Wheat is the second most important direct source of food calories in the world. After considerable improvement during the Green Revolution, increase in genetic yield potential appears to have stalled. Improvement of photosynthetic efficiency now appears a major opportunity in addressing the sustainable yield increases needed to meet future food demand. Effort, however, has focused on increasing efficiency under steady-state conditions. In the field, the light environment at the level of individual leaves is constantly changing. The speed of adjustment of photosynthetic efficiency can have a profound effect on crop carbon gain and yield. Flag leaves of wheat are the major photosynthetic organs supplying the grain of wheat, and will be intermittently shaded throughout a typical day. Here, the speed of adjustment to a shade to sun transition in these leaves was analysed. On transfer to sun conditions, the leaf required about 15 min to regain maximum photosynthetic efficiency. *In vivo* analysis based on the responses of leaf CO_2 assimilation (A) to intercellular CO_2 concentration (c_i) implied that the major limitation throughout this induction was activation of the primary carboxylase of C3 photosynthesis, ribulose-1,5-bisphosphate carboxylase/oxygenase (Rubisco). This was followed in importance by stomata, which accounted for about 20% of the limitation. Except during the first few seconds, photosynthetic electron transport and regeneration of the CO_2 acceptor molecule, ribulose-1,5-bisphosphate (RubP), did not affect the speed of induction. The measured kinetics of Rubisco activation in the sun and de-activation in the shade were predicted from the measurements. These were combined with a canopy ray tracing model that predicted intermittent shading of flag leaves over the course of a June day. This indicated that the slow adjustment in shade to sun transitions could cost 21% of potential assimilation.

This article is part of the themed issue 'Enhancing photosynthesis in crop plants: targets for improvement'.

1. Introduction

Leaves of crops in the field experience frequent fluctuations in light, moving from shade to full sunlight, and vice versa, as clouds obscure the sun or as leaves go into the shade of other leaves, stems and floral structures. Recently, it was shown that increasing the rate at which leaves could re-adjust photosynthetic efficiency on transfer to shade increased productivity of a tobacco crop in replicated field trials by 14–20% [1]. This was shown to result from a decrease in the time required for non-photochemical quenching to relax and the efficiency of leaf photosynthetic CO_2 uptake (A), in limiting light, to recover. Equally, there is a lag in achieving maximum efficiency when leaves are transferred in the opposite direction from shade to sun. The increase in A that occurs following the transition has been termed photosynthetic induction [2]. Although many factors could govern the speed of induction, it has been shown to correlate with, and modelled

to correspond to, Rubisco activation in, for example, soya bean and tobacco [3,4]. More recently, over-expression of *Rca*, the gene coding for Rubisco activase (Rca), in rice resulted in a slightly increased speed of induction at 25°C [5]. *In vivo*, the steady-state response of leaf CO_2 uptake (A) to intercellular CO_2 concentration (c_i) has proved a highly valuable means to partition limitations, including apparent Rubisco activity ($V_{c,max}$). Recently, this concept has been extended by inducing photosynthesis on the same leaf in a range of CO_2 concentrations. This allowed the production of dynamic A/c_i responses to infer limitations at different stages of induction in soya bean. On transfer of leaves from a shade light level of 100 μmol m^{-2} s^{-1} to a full sun level of 2000 μmol m^{-2} s^{-1}, 10–20 min were required for leaves to regain full efficiency. The dynamic A/c_i analysis over this period inferred that the slowest responding determinant of photosynthetic rate was Rubisco activity, suggesting activation of this enzyme as the primary cause of this delay [3,4]. However, the impact this might have on production was not quantified.

Bread wheat (*Triticum aestivum* L.) is second only to rice in importance to the world's population as a direct source of food calories [6]. After large improvements in global yields of wheat per hectare following the Green Revolution, improvement stagnated in the first decade of this century [6–9]. Improved partitioning of biomass to grain, i.e. harvest index, was roughly doubled, making it the key factor of genetic improvement of yield potential during the Green Revolution. Harvest index is now at about 60% of total shoot biomass in contemporary cultivars, and is close to its biological limits [10,11]. This may explain why increases in yield potential have been stagnating in recent years. New innovations are therefore needed if genetic yield potential of wheat is to be improved further [10,12]. Photosynthetic efficiency in wheat, as in all crops, falls well short of its theoretical potential and has been improved little with selection and breeding [13]. Indeed some have argued that leaf photosynthetic capacity has decreased with domestication [14].

The flag leaf of wheat, together with the ear, are considered to account for most of the carbohydrate that accumulates in the developing grain [15]. Furthermore, the proportion of photosynthate derived from the flag leaf relative to the ear has increased progressively with the increase in harvest index through the past 50 years [16], so increasing its importance as a source of carbohydrate for the developing grain. Using a current cultivar of wheat, this study: (i) determines the speed of adjustment of photosynthesis in the flag leaf on transfer from shade to sun; (ii) infers, by developing dynamic A/c_i responses, the *in vivo* factors determining the speed of adjustment; and (iii) estimates the loss of potential production that may result from this slow adjustment.

2. Material and methods

(a) Plant material and growth conditions

A bread-making quality wheat (*Triticum aestivum* L.) cv. Highbury was used (Nottingham University, UK). Seed was sown into 3 l containers of soil-less compost mix (Petersfield Products, Leicester, UK) incorporating a broad range fertilizer (PG Mix, Yara, Grimsby, UK), in a controlled environment greenhouse. Day/night temperatures were maintained at 24 ± 9.3°C/19 ± 1.4°C (mean ± s.d.) and relative humidity was 45 ± 12.6%. Growth CO_2 concentration in the greenhouse air was measured hourly and averaged 449 ± 23 μmol mol^{-1} over the duration of the experiment. Daylight was supplemented with high pressure sodium lamps (SON-T 400 W, Philips Lighting, Eindhoven, The Netherlands) to ensure a minimum photosynthetic photon flux density (PPFD) of 500 μmol m^{-2} s^{-1} at the plant surface for 16 h d^{-1}. After germination, seedlings were thinned to one per container. Containers were watered daily to field capacity.

(b) Gas exchange and analysis of photosynthetic CO_2 responses

Photosynthetic gas exchange of fully emerged flag leaves was measured between heading and anthesis. The mid-section of the leaf was enclosed within a controlled environment cuvette integrated into a portable gas exchange system incorporating infrared CO_2 and water vapour analysers (LI-6800F, LI-COR, Lincoln, NE). Light was provided through the light-emitting diodes incorporated into the cuvette head.

Response curves of net leaf CO_2 uptake (A) to PPFD were determined to obtain preliminary values for day respiration (R_d) and identify the lowest PPFD that would be saturating for subsequent static and dynamic A/c_i analysis. In all measurements, leaf temperature was maintained at 25°C and leaf vapour pressure deficit (VPD_{leaf}) at *ca* 1.0 kPa. Transpiration was measured simultaneously to determine stomatal conductance to water ($g_{s,w}$), to correct for impacts on measured CO_2 fluxes, and to allow calculation of c_i based on transpiration-corrected leaf conductance to CO_2. Leaves were induced to steady state at a cuvette CO_2 of 400 μmol mol^{-1} and a PPFD of 1500 μmol m^{-2} s^{-1}, allowing at least 40 min for steady state to be achieved. PPFD was then stepped down through 1200, 1000, 800, 600, 500, 400, 300, 200, 150, 100, 50 and 0 μmol m^{-2} s^{-1}; measurements were collected immediately cuvette conditions stabilized at each light level. The response of A to incident PPFD was then fit using nonlinear least squares (*nls*: R Language and Environment) to a non-rectangular hyperbola [17]:

$$A = \frac{\phi I + A_{sat} - \sqrt{(\phi I + A_{sat})^2 - 4\theta\phi I A_{sat}}}{2\theta} - R_d,$$

where ϕ is the realized quantum yield (mol mol^{-1}); I, incident PPFD (μmol m^{-2} s^{-1}); A_{sat}, the maximum gross rate of leaf CO_2 assimilation (μmol m^{-2} s^{-1}); θ, a dimensionless curvature parameter; R_d, the daytime rate of respiration (μmol m^{-2} s^{-1}). Fitted values were (mean ± s.e.): ϕ, 0.067 ± 0.0049; A_{sat}, 38.1 ± 3.58; θ, 0.58 ± 0.044; R_d, 1.68 ± 075; R_d was used as an initial value in models of the photosynthetic response to CO_2 concentration.

The 'static' response of A to c_i (expressed as the mole fraction in air: μmol mol^{-1}) was determined by obtaining steady-state A under the conditions described above, but by maintaining PPFD at 1200 μmol m^{-2} s^{-1} and varying CO_2 in the air surrounding the leaf (c_a). Measurements were made at 430, 300, 200, 150, 100, 50 and approximately 0 μmol mol^{-1} c_a, which was then increased to 430, 500, 600, 800 and 1000 μmol mol^{-1}; following procedures recommended previously [18]. Values for A and c_i were calculated from the equations of Farquhar & von Caemmerer [19].

Parameters of the response of A to c_i were characterized on the basis of limitation by Rubisco (A_C) and electron transport (A_J) [19].

$$A_C = V_{c,max}\left(\frac{c_i - \Gamma^*}{c_i + K_C(1 + O/K_O)}\right) - R_d$$

and

$$A_J = J\left(\frac{c_i - \Gamma^*}{4.5c_i + 10.5\Gamma^*}\right) - R_d.$$

The maximum rate of carboxylation ($V_{c,max}$, μmol m^{-2} s^{-1}), the rate of electron transport (J, μmol m^{-2} s^{-1}), and R_d were fit

using nonlinear least squares. To do this, values for: Γ^*, the photorespiratory compensation point; K_C, the Rubisco Michaelis constant for CO_2; and K_O, the Rubisco Michaelis constant for O_2, were calculated at the mean leaf temperature, based on values for tobacco following Bernacchi *et al*. [20]. Using nonlinear least squares, $V_{c,max}$ and R_d were estimated first, and the value of R_d was used when estimating J. Parameters were normalized to 25°C following previously described relationships to temperature [20]. Because calculation of the true $V_{c,max}$ requires determination of c_c, we note that the term determined here from c_i and referred to as $V_{c,max}$ is determined by both the *in vivo* activity of Rubisco and mesophyll conductance (g_m).

To identify the transition point between Rubisco and ribulose-1,5-bisphosphate (RuBP) limitation, we used an approach derived from the recommendations of Gu *et al*. [21]. All possible combinations of A_C and A_J were fit to each CO_2 response curve, and the best fit was selected based on the minimal value of

$$\sum_{i=1}^{nC} (\hat{A}_{Ci} - A_{Ci})^2 + \sum_{i=1}^{nJ} (\hat{A}_{Ji} - A_{Ji})^2$$

where $\hat{A}$ are predicted, and A observed values for the respective segments of the A/c_i curves. The best fitting A_C, A_J combination was considered admissible if the transition point predicted fell between data assigned to A_C and A_J. Stomatal limitation (l) was also calculated from the A/c_i response [22],

$$l = \frac{A_{c_a} - A_{c_i}}{A_{c_a}},$$

where A_{c_a} is the value of A as determined from the A/c_i response if $c_i = c_a$, i.e. assuming infinite boundary layer and stomatal conductances. A_{c_i} is the actual A achieved at the given c_a, i.e. accounting for the decrease in c_i resulting from the actual stomatal conductance (g_s).

To determine the limitations to A during low to high light transitions leaf gas exchange was measured at a range of c_a and 'dynamic' A/c_i responses constructed as described previously [24]. At the start of measurements each leaf was brought to steady state at a c_a of 400 µmol mol^{-1}, PPFD of 1200 µmol m^{-2} s^{-1}, cuvette air temperature of 25°C, and VPD *ca* 1.0 kPa. Induction measurements followed decreases in PPFD to 50 µmol m^{-2} s^{-1} for 30 min (shade): gas exchange was recorded at 10 s intervals for 15 min following a step change back to 'sun' (1200 µmol m^{-2} s^{-1} PPFD), a PPFD sufficient for saturation of $V_{c,max}$ and J. The cycle of 30 min shade + 10 min sun was repeated at c_a of 50, 100, 200, 300, 400, 500, 600, 800 and 1000 µmol mol^{-1}. Within a few seconds after the transition from 'shade' to 'sun', leaf temperatures rose by approximately 1°C to the range 24.5–25.1°C, with coefficients of variation (CV) during inductions less than 0.63%. The range of leaf VPD during inductions was 1.0–1.2 kPa, with CV < 2.8%; CV for c_a were less than 3%. In the shade at ambient and higher cuvette c_a, g_s decreased, minimizing the range of c_i that could be obtained and preventing characterization of A_J. To fully characterize photosynthetic limitations during induction dynamic A/c_i measurements were repeated, but using a c_a of 100 µmol mol^{-1} during shade to inhibit stomatal closure before switching to the desired c_a and sun condition for induction.

CO_2 response curves were fit to the data for each 10 s interval of induction. A small number of inadmissible fits were obtained when there was insufficient data to fit both A_C and A_J; we re-fit these cases using either A_C or A_J (alongside R_d), and chose the best fit based on a comparison of $\sum_{i=1}^{N} (\hat{A}_{Ci} - A_{Ci})^2$ and $\sum_{i=1}^{N} (\hat{A}_{Ji} - A_{Ji})^2$. To determine whether A during photosynthetic induction was limited primarily by $V_{c,max}$ or J, parameters from the dynamic A/c_i responses were used in combination with steady-state $g_{s,w}$ to estimate a maximum probable operating c_i: $(g_{s,w}/1.64)(c_a - c_i)$ equated to $V_{cmax}((c_i - \Gamma^*)/(c_i + K_{CO})) - R_d$. The resulting quadratic was solved for c_i at each 10 s interval through induction.

(c) *In vivo* kinetics for Rubisco activation in wheat

The time constant for Rubisco activation was determined from the kinetics of A following transitions from low to high light, excluding transient changes occurring during the first minute as described previously [23]

$$A^* = A_f^* - (A_f^* - A_i)e^{-t/\tau}$$

where A_f^* is a steady-state value for A^*: the potential gross leaf CO_2 assimilation in sun, corrected to constant c_i. A^* was calculated as $(A + R_d)(c_{i,f}/c_i)$, where $c_{i,f}$ is the steady-state c_i approximated as $0.65c_a$, and R_d was assumed to be 1.6 µmol m^{-2} s^{-1} (the fitted value from our steady-state A/c_i response). A_i is the gross assimilation extrapolated to $t = 0$, which provides an estimate of initial Rubisco activation [3,23]. Finally, τ is the time constant for recovery of photosynthesis. The model was fit using both nonlinear least squares (using data collected from 60 s until 600 s after the change in PPFD), and the linear regression technique described previously [23], where a plot of $\ln(A_f^* - A^*)$ against time has slope $-1/\tau$ and intercept $\ln(A_f^* - A_i)$. The same model was fit to A^* and $V_{c,max}$, allowing a novel comparison between estimates of τ for Rubisco activation based on A^* and $V_{c,max}$.

To obtain integrated CO_2 assimilation ($\overline{A^*}$) during increases in PPFD, if it is assumed that RuBP concentration is saturating, the model can be re-written as [24]

$$\overline{A^*} = A_f^* t - (A_f^* - A_i)\tau + (A_f^* - A_i)\tau e^{-t/\tau}.$$

Setting $\tau = 0$ estimates potential assimilation rate with a square response to PPFD ($\overline{A^*}_{max} = A_f^* t$), and an estimate of foregone assimilation is $\overline{A^*}_{max} - \overline{A^*}$. To determine the impacts of Rubisco kinetics on CO_2 assimilation, the response of $\overline{A^*}$ to PPFD was modelled at approximately 60 s time intervals during a diurnal period. A PPFD regime was used that predicted light available to the second layer of a crop canopy [25]. This is justified by the observation that the ears represent the first layer and cause intermittent shading of the flag leaves as the angle of the sun progresses through the day. In the data used, PPFD at a point on the leaf had been predicted using reverse ray tracing, with shade-generating structures in the canopy distributed at random within each layer. A clear sky day in June at latitude 44°N had been assumed for calculating sun angles over the course of the day [25]. To model gross photosynthesis throughout the diurnal period, initial photosynthesis for each approximately 60 s interval (A_i) was taken to be A^* predicted for the preceding interval, except at first light where A_i was assumed to be zero. The potential maximum gross rate of photosynthesis during each timestep (A_f^*) was predicted as $(\phi I + A_{sat} - \sqrt{(\phi I + A_{sat})^2 - 4\theta\phi I A_{sat}})/2\theta$, using parameters from the PPFD response curves fit to steady-state data and setting t = duration of the timestep (s). When PPFD was increasing we set τ to 180 s, the mean value determined by substituting the time-series of $V_{c,max}$ from our dynamic A/c_i analysis into the induction model: $V_{c,max} = V_{c,max,f} - (V_{c,max,f} - V_{c,max,i})e^{-t/\tau}$. When PPFD was decreasing, we estimated $\overline{A^*}$ as $A_f^* t$, and predicted A_i as above, but using $\tau = 300$ s for the rate of decrease towards the lower A_f^* predicted from PPFD. The value of $\tau = 300$ s for the decrease was predicted on the basis that 30 min 'shade' treatment resulted in a decrease in $V_{c,max}$ from $V_{c,max,f}$ to $V_{c,max,i}$.

3. Results

(a) Factors limiting photosynthesis in wheat, cv. Highbury: steady state

Responses to light and CO_2 measured from steady-state photosynthesis indicated high maximum net leaf CO_2

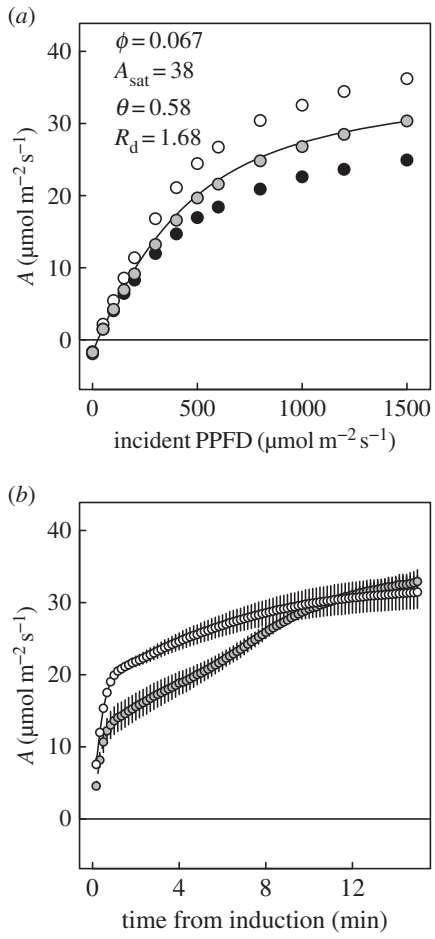

Figure 1. Responses of photosynthetic CO_2 uptake (A) to PPFD in flag leaves of bread-wheat at heading-anthesis. (*a*) Static light-response: solid line indicates light response based on means of fitted parameters shown, symbol shading differentiates three plants used in the experiment. (*b*) Dynamics of photosynthetic induction following a transition from 50 to 1200 μmol m^{-2} s^{-1} PPFD (shade to sun): values are means ± s.e. based on three leaves from separate plants, shaded symbols and dashed lines indicate leaves maintained at 400 μmol mol^{-1} [CO_2] during the preceding 30 min shade period, open symbols and solid lines indicate leaves maintained at 100 μmol mol^{-1} [CO_2] during the preceding 30 min shade period.

assimilation rates ($A_{sat} > 30$ μmol m^{-2} s^{-1}; figures 1 and 2), with saturation approached at a PPFD of about 1200 μmol m^{-2} s^{-1} (figure 1*a*). This was the subsequent level chosen as a proxy for 'sun' conditions in examining induction. On transfer from 'shade' (50 μmol m^{-2} s^{-1}) to 'sun' at c_a of 400 μmol mol^{-1} there was an initial rapid increase in A (figure 1*b*), followed by a slower increase lasting *ca* 15 min. When leaves were maintained at a c_a of 100 μmol mol^{-1} in the shade to prevent stomatal closure, then exposed to 'sun' at c_a 400 μmol mol^{-1}, the initial transient increase in A saturated at a higher value, indicating a decrease in stomatal limitation; however, after 10 min A was similar in the two experiments (figure 1*b*).

Static A/c_i responses showed that at steady state, limitation of A_{sat} was consistent with A_C (figure 2); $c_{i,trans}$, the transition from limitation by A_C, with $V_{c,max}$ (113 ± 13 μmol m^{-2} s^{-1}; mean ± s.e., $N = 3$), to limitation by A_J, with J (214 ± 18 μmol m^{-2} s^{-1}), occurred at 407 ± 27 μmol mol^{-1}. This transition was therefore well above the operating c_i, i.e. that obtained at the current atmospheric level of 400 μmol mol^{-1} and above the c_i that would be obtained under the slightly elevated ambient c_a in the greenhouse of 449 μmol mol^{-1}

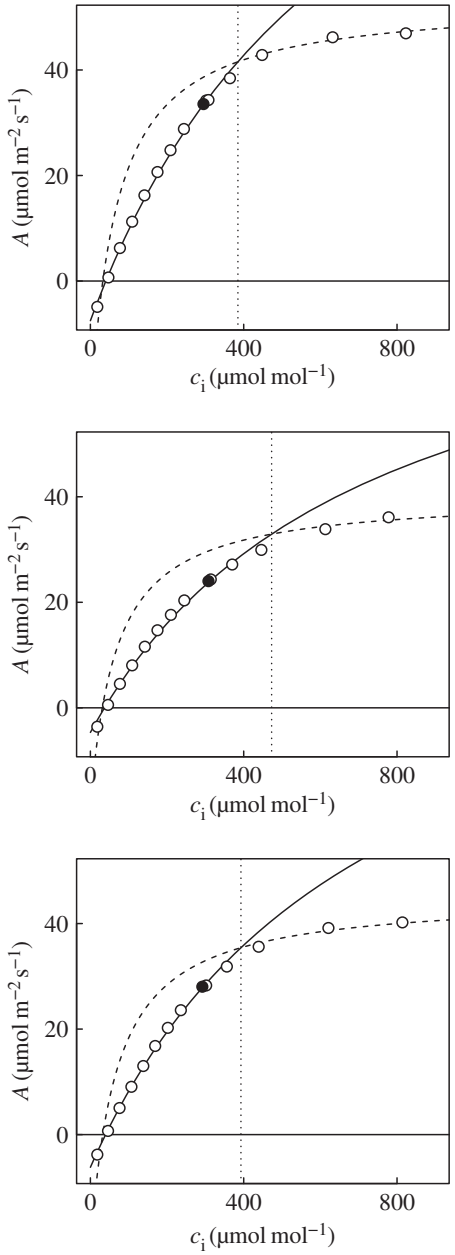

Figure 2. Response of net leaf CO_2 uptake (A) to intercellular CO_2 concentrations (c_i) in flag leaves of wheat at heading-anthesis. Fitted curves are shown for Rubisco-limited photosynthesis (solid lines) and RuBP-limited photosynthesis (dashed lines). Vertical dotted lines indicate the c_i at which limitation of photosynthesis transitions from Rubisco to RuBP regeneration ($c_{i,trans}$), and filled points the steady-state operating values. Parameter values were (mean ± s.e., $N = 3$): $V_{c,max} = 113 \pm 12.7$ μmol m^{-2} s^{-1}; $R_d = 1.6 \pm 0.31$ μmol m^{-2} s^{-1}; $J = 214 \pm 18.3$ μmol m^{-2} s^{-1}; $\Gamma = 39.0 \pm 1.00$ μmol mol^{-1}; $c_{i,trans} = 407 \pm 27.4$ μmol mol^{-1}. Conditions during measurements for each leaf were as follows (mean, CV < 0.01): vapour pressure deficit, 0.99 kPa; photosynthetic photon flux density, 1200 μmol m^{-2} s^{-1}; leaf temperature, 25°C.

(figure 2). Stomatal limitation to A_{sat} at 400 μmol mol^{-1} c_a (l) was 0.196 ± 0.010 (mean ± s.e.), i.e. if there was no diffusive barrier at the epidermis A_{sat} would be about 20% higher.

(b) Factors limiting photosynthesis in wheat, cv. Highbury: during induction

A/c_i responses constructed for each 10 s interval of induction following transition from 50 to 1200 μmol m^{-2} s^{-1} PPFD (electronic supplementary material, figure S1) showed several

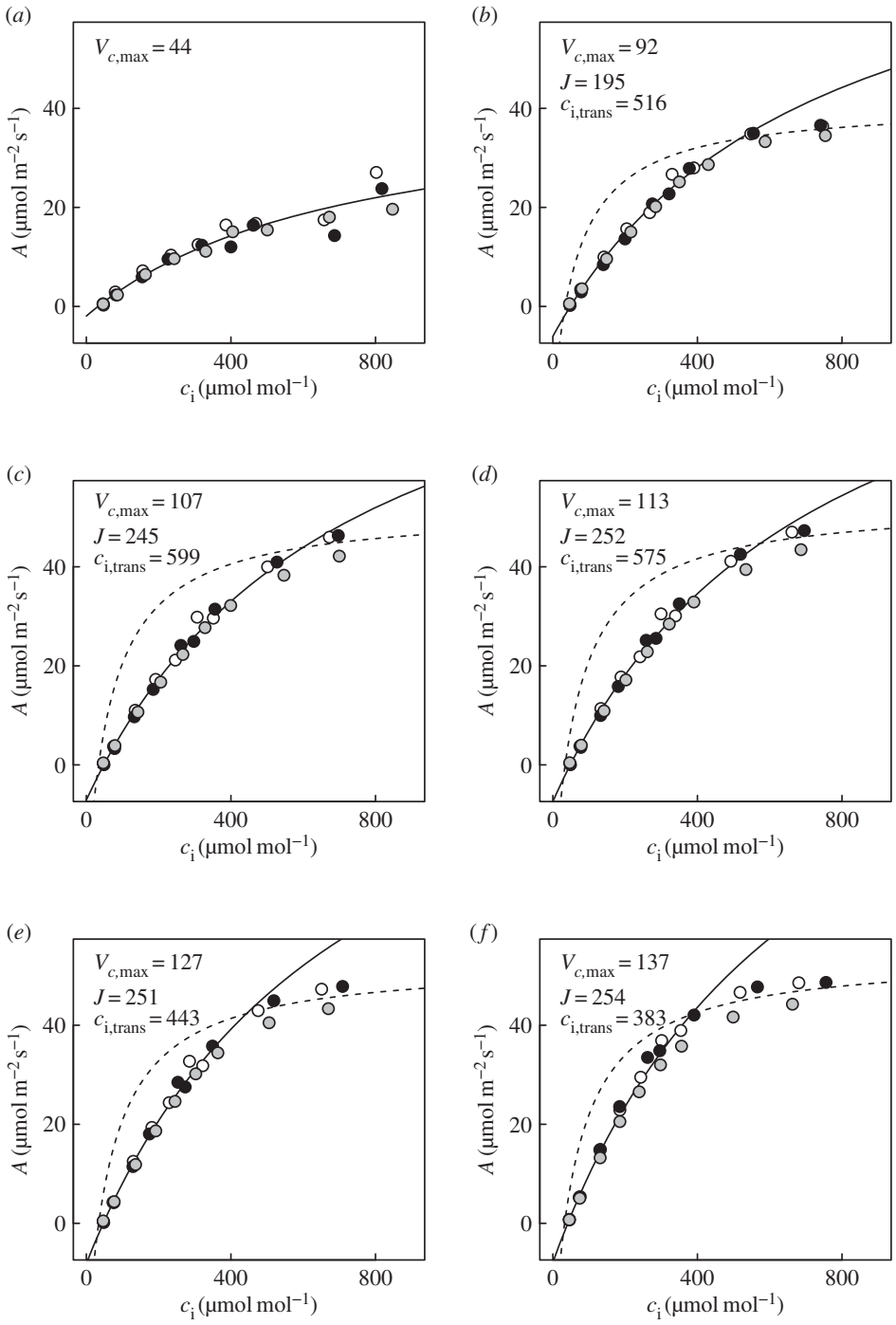

Figure 3. Photosynthetic induction after transition from 50 to 1200 μmol m^{-2} s^{-1} PPFD, represented by dynamic A/c_i analysis at: (*a*) 20 s; (*b*) 1 min; (*c*) 2.5 min; (*d*) 3 min; (*e*) 4.5 min; (*f*) 10 min.

phases of photosynthetic limitation. Admissible, best fitting models during the first 40 s after the transition to sun, consisted in most cases solely of limitation by A_C, with $V_{c,max}$ at less than 40% of its steady-state value (compare figures 2 and 3*a*). However, sums of squares (SS) for residuals of models fit as a single limitation phase were relatively high (6.97–37.91); stronger fits were obtained when both A_C and A_J could be identified (figure 3*b–f*; SS, 1.04–12.29).

Initially, both $V_{c,max}$ and J increased, but J increased more rapidly than $V_{c,max}$, so $c_{i,trans}$ rose to a maximum approaching 600 μmol mol^{-1} at around 2.5 min (figure 3*b*,*c*). At 3 min, J saturated close to 250 μmol m^{-2} s^{-1} and $c_{i,trans}$ began to decrease as $V_{c,max}$ slowly rose (figure 3*d*). For the remainder of the first 10 min following the transition, decreases in $c_{i,trans}$ continued, in concert with increasing $V_{c,max}$. The increase in $V_{c,max}$ was most rapid in the first 4.5 min (figure 3*e*), and adjustment continued through to 10 min (figure 3*f*). After this time, A/c_i responses were comparable with those measured at steady state (figures 2 and 3*f*).

Time series for $V_{c,max}$, J and $c_{i,trans}$ (figure 4) developed from data including those shown in figure 3, provided a τ for $V_{c,max}$ of *ca* 3 min (mean ± s.e.m., 181 ± 12.8 s), more than three times that for J (50.1 ± 1.91 s); slow adjustment in $V_{c,max}$ clearly had a strong effect on $c_{i,trans}$ between 2.5 and 10 min into the induction (figure 4). Calculation of a maximum probable operating c_i (figure 4; based on A/c_i responses and steady state $g_{s,w}$) further demonstrated that $c_{i,trans}$ exceeded this value throughout the period of induction, confirming that in our analysis apparent $V_{c,max}$ was the dominant biochemical variable limiting photosynthesis

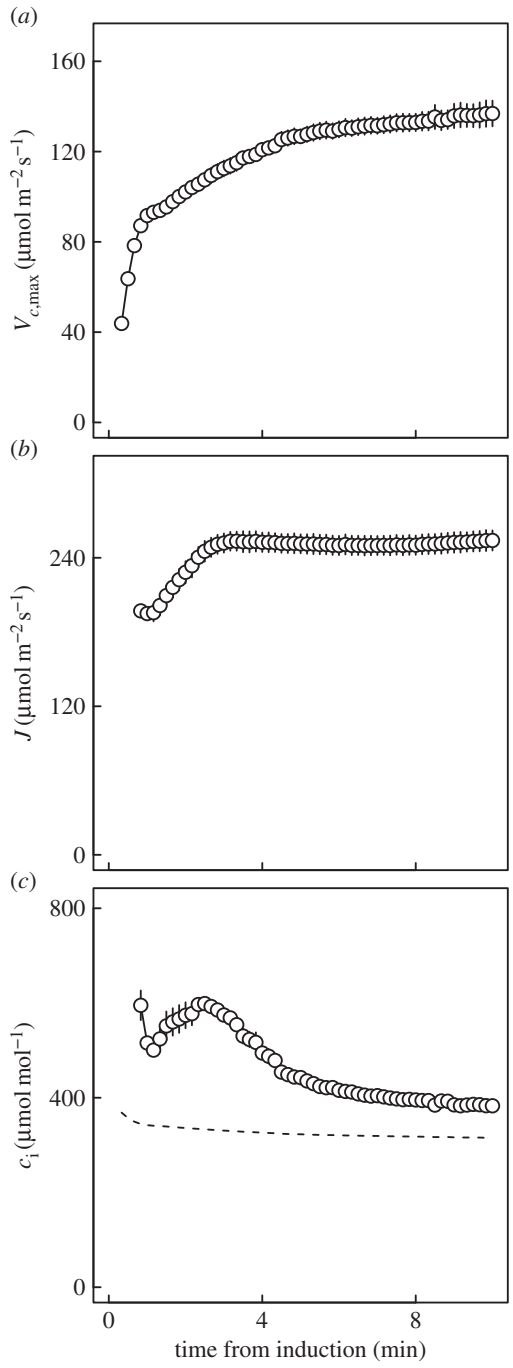

Figure 4. Dynamics of photosynthetic limitations affecting wheat leaves over 10 min following a step change in PPFD from 50 to 1200 μmol m^{-2} s^{-1} (shade to sun). (*a*) Maximum rate of Rubisco carboxylation ($V_{c,max}$). (*b*) Rate of electron transport (J). (*c*) The c_i at which the primary limitation imposed on photosynthesis switches between $V_{c,max}$ and J ($c_{i,trans}$). Values are means ± s.e. based on three leaves from separate plants (indicated by symbol shading). The dashed line in (*c*) places an upper limit on operating c_i, assuming a chamber [CO_2] (c_a) of 400 μmol mol^{-1}, and steady-state stomatal conductance of 0.7 mol m^{-2} s^{-1}.

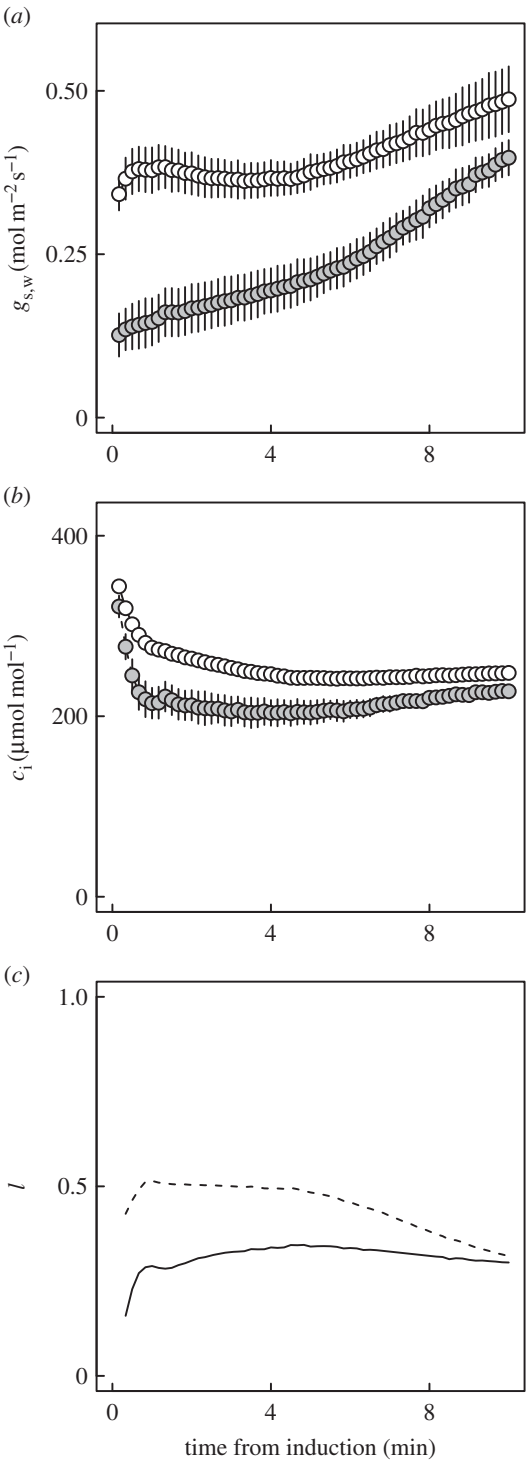

Figure 5. Stomatal effects following a step change in PPFD from 50 to 1200 μmol m^{-2} s^{-1}, as affected by [CO_2] pre-treatment. (*a*) Stomatal conductance to water vapour ($g_{s,w}$). (*b*) Intercellular CO_2 concentrations (c_i). Values are means ± s.e. based on three leaves from separate plants. (*c*) Limitation imposed by stomata (l), relative to infinite conductance at [CO_2] = 400 μmol mol^{-1}. Shaded symbols and dashed lines are for 400 μmol mol^{-1} [CO_2] during shade; open symbols and solid lines are for 100 μmol mol^{-1} [CO_2] during shade.

through the induction (figure 4*c*). Comparisons of τ for $V_{c,max}$ with estimates of τ for Rubisco activation effects on photosynthesis based on A^* suggested a range of values for τ between 3 and 4 min (electronic supplementary material, figure S2).

Shading, such as that simulated by our 50 μmol m^{-2} s^{-1} PPFD pre-treatment, affects stomatal opening. To characterize A_J using dynamic A/c_i analysis, it was necessary to increase stomatal conductance following shade by decreasing c_a during the low-light pre-treatment. Compared with plants pre-treated at 400 μmol mol^{-1} c_a, during the first 4 min after illumination both A and $g_{s,w}$ of plants pre-treated at c_a = 100 μmol mol^{-1} were higher by 30–65% (figure 1*b*) and 88–171% (figure 5*a*), respectively, resulting in an increase in cumulative net CO_2 assimilation of 22%. Pre-treatment with a c_a of 100 μmol mol^{-1} also resulted in progressive decreases in c_i through the induction, suggesting increasing

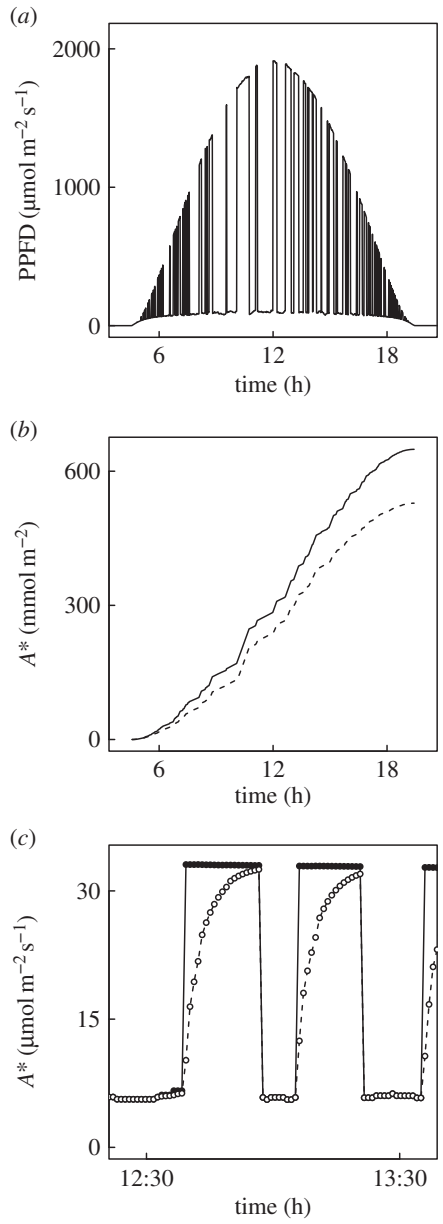

Figure 6. (*a*) The simulated course of photon flux (PPFD) on a clear sky June day at latitude 44°N for a point on the flag leaf, assuming one layer of randomly distributed elements above the leaf [25]. (*b*) The cumulative gross assimilation of CO_2 assuming that A^* instantaneously adjusts to the steady-state value fit to the light response curve (figure 1*a*), i.e. no lag on a shade to sun transition (solid line); versus accounting for the lag imposed by Rubisco re-activation (dashed line). (*c*) As for (*b*) but showing instantaneous A^* for the period around solar noon for the no-lag scenario (filled symbols) and the scenario modelled on measured Rubisco activation (open symbols).

photosynthetic efficiency was a key control on c_i (figure 5*c*). Pre-treatment at $c_a = 400$ μmol mol^{-1} resulted in rapid declines of c_i to a minimum that was maintained for around 5 min before c_i started to increase (figure 5*b*). In both cases, after 10 min c_i remained below values expected at steady state (figures 2 and 4*c*); slow relaxation of stomatal limitation affected c_i over considerably longer periods than relaxation of limitation by $V_{c,max}$. Immediately after PPFD increased, l in leaves pre-treated at a $c_a = 400$ μmol mol^{-1} CO_2 was twice as high as in leaves treated at 100 μmol mol^{-1}, reaching a maximum of 0.5. After 10 min l was similar between the two treatments (figure 5*d*), but remained 50% higher than for steady state A/c_i responses in both cases (400 μmol mol^{-1}, 0.32; 100 μmol mol^{-1}, 0.3).

(c) Impact of induction characteristics on diurnal photosynthesis

Simulation of PPFD fluctuations that would occur at a single point on a flag leaf due to intermittent shading from ears and other flag leaves on a clear sky summer day, shows multiple transitions from shade to sun and back to shade (figure 6*a*). Based on the response of A to PPFD determined for these leaves (figure 1*a*), the cumulative assimilation of CO_2 over the course of a clear sky day, accounting for the fluctuations in PPFD, is shown in the upper line of figure 6*b*. The total uptake of CO_2 over the daylight hours is 640 mmol m^{-2}. When account is taken of de-activation of Rubisco, depending on duration of the 'shade' period and then subsequent re-activation, cumulative CO_2 assimilation would follow the lower line. This reaches a total of 506 mmol m^{-2} or a 21% reduction due to the slow recovery of photosynthetic efficiency, due to the re-activation of Rubisco, following shade to sun transitions. The dynamics of this loss may be seen more clearly from a narrower time window around solar noon. Here, for instantaneous assimilation rates the area above the dotted line and below the solid line represents lost assimilation (figure 6*c*).

4. Discussion

On shade to sun transitions, this study has shown that several minutes are required for the wheat flag leaf to re-attain maximum photosynthetic efficiency (figure 1*b*). At the level of leaf biochemical limitations, the apparent maximum activity of Rubisco ($V_{c,max}$) limits this rate of induction, implying activation of this enzyme as the key factor, rather than regeneration of the RuBP CO_2 acceptor molecule (J). This was clearly indicated by the fact that $c_{i,trans}$ was well above the actual c_i when c_a was at the current atmospheric level of 400 μmol mol^{-1} and at the actual greenhouse growth c_a of 449 μmol mol^{-1} (figures 3 and 4*c*). In contrast to previous studies [4], stomatal limitation plays a role in the speed of induction, declining from *ca* 0.5 in the first 3 min to about 0.3 at steady state, indicating that about 20% of the lag is due to stomatal movement (figure 5*c*). This is also indicated by the fact that when the leaf is at the ambient c_a of 400 ppm throughout, c_i declines to about 200 μmol mol^{-1} before recovering to *ca* 230 μmol mol^{-1} at steady state (figure 5*b*). Combining the ray tracing model of Zhu *et al*. [25] and the modelled kinetics of Rubisco de-activation and activation on sun-to-shade-to-sun transitions following Woodrow *et al*. [3,23,24], losses due to the slow induction were calculated. Parametrized on the data reported here for wheat flag leaves, the lag in activation of Rubisco following shade to sun transitions resulted in a 21% loss of potential flag leaf assimilation (figure 6).

The findings (figures 3 and 4*c*) indicate $V_{c,max}$, or the apparent maximum activity of Rubisco, as the major factor limiting the rate of induction, implying the speed of re-activation of Rubisco. This is consistent with previous studies of tobacco, rice and soya bean [3–5]. However, the apparent $V_{c,max}$ calculated from the A/c_i response is also affected by mesophyll conductance (g_m). [CO_2] at Rubisco (c_c) will be less than c_i due to mesophyll conductance. If g_m increased

during the course of induction, it would cause part of the apparent increase in $V_{c,max}$. As a physical conductance, g_m would not vary. However, modelling suggests that in reality it will have some dependence on the positioning of organelles, and in particular the relative localization of chloroplasts and mitochondria, which may change in response to light levels within the leaf [26–28]. It is known that chloroplasts may alter their position with PPFD. Through its impact on g_m, this movement could explain some, but certainly not all, of the change in apparent $V_{c,max}$ [28]. Transporters and channels in membranes may change dynamically to affect g_m. Therefore, the lag attributed to Rubisco activation could in reality be a combination this activation with an increase in g_m.

Previous research has shown a strong correlation between the speed of induction and the activation of Rubisco, in particular, the enzyme Rubisco activase [3,5]. Also, as noted above, in contrast to a previous dynamic analysis of A/c_i responses in induction in soya bean [4], stomata limit the speed of induction, accounting for about 20% of the change (figure 5). However, stomatal opening appears to depend strongly on photosynthesis in the mesophyll [29,30]. Thus, there may be some dependency of the speed of stomatal opening on the speed of Rubisco activation in the mesophyll. Assuming c_c in the shade is sufficient to support rapid carbamylation of Rubisco, increasing the speed of activation might increase the speed of stomatal opening.

The dynamic A/c_i method used to identify photosynthetic limitations in this study has been developed recently [4]. In this study, we found that it was necessary to decrease c_a in the 'shade' in order to limit stomatal closure that otherwise prevented characterization of A_J in wheat. We anticipate that this technical solution will not have had a substantial effect on Rubisco activation independent of the 'shade' because at low light photosynthesis will be entirely limited by RuBP regeneration not Rubisco, and because c_i remained high. Decreases in activation linked with de-carbamylation as a result of low CO_2 availability [31] are unlikely in this scenario. Perhaps more importantly, dynamic A/c_i analyses are intended to capture non-steady state dynamics, and do so by characterizing induction at a range of c_a. The rate of Rubisco activation during induction is thought to respond to CO_2 availability [32], consistent with greater availability of CO_2 driving Rubisco carbamylation and minimizing alternative reactions (reviewed in [33]). The timed snapshots obtained using dynamic A/c_i analysis, in strict terms, violate the usual assumption made when using the Farquhar *et al*. model [34] that Rubisco activity is at steady state. Calculating $V_{c,max}$ in a dynamic analysis averages across measurements that may reflect different activation states. It is also possible that the eventual steady state of activation during each induction will depend on c_a, but evidence suggests decreases in activation under light saturated conditions are usually observed only when c_i is significantly below 100 µmol mol^{-1}, and then only in certain species [31]. Nonetheless, specific parameter values for dynamic A/c_i response curves should be interpreted with some caution. The usefulness of the dynamic A/c_i analysis is primarily as a mean of assessing the sequence and approximate timing of transitions between different photosynthetic limitations during induction. We anticipate that experimentation and modelling to understand how c_a affects Rubisco activation state during induction will improve our understanding of the induction process, and the potential feedbacks due to mesophyll and stomatal conductance responses.

Importantly, this research shows that the speed of non-steady-state adjustment of photosynthesis to light fluctuations in the field, regardless of underlying cause, will strongly affect flag leaf photosynthesis. In turn, this will decrease the supply of assimilate for the developing grain. Although, only the flag leaf was examined here, the same lags in induction will likely apply to all leaves of the plant. Thus, the growth and production that supports the development of the plant to flowering and seed fill will be affected. Increasing the rate of induction following shade to sun transitions under typical field conditions during grain filling would decrease the impact of a significant limitation, and therefore represents an excellent target through which increases in productivity would be obtained. The gains in productivity could be of similar magnitude to those observed by bioengineering a faster rate of adjustment to sun to shade transitions [1]. Acceleration might be achieved by over-expressing the amount of Rca [5], by targeted amino acid substitutions of Rca [35], altered ratios of alpha and beta forms [35], or by exploring the natural variation in speed of adjustment apparent in soya bean [4]. The results presented here suggest that these changes have the potential to open an important new route, through photosynthesis, to a much needed yield jump for wheat.

Data accessibility. The datasets supporting this article are available from Lancaster University: doi:10.17635/lancaster/researchdata/144.

Authors' contributions. S.H.T. and S.L. designed experiments and statistical analyses, and co-wrote the article; S.H.T. carried out measurements.

Competing interests. We have no competing interests.

Funding. Lancaster University provided the financial support necessary to undertake this work.

Acknowledgements. We thank Dr Elizabete Carmo-Silva for helpful discussions on Rubisco activation and for supplying us with the wheat plants used here, and we thank Prof. Xinguang Zhu for providing raw data on light within canopies from his simulation study [25].

References

1. Kromdijk J, Glowacka K, Leonelli L, Gabilly ST, Iwai M, Niyogi KK, Long SP. 2016 Improving photosynthesis and crop productivity by accelerating recovery from photoprotection. *Science* **354**, 857–861. (doi:10.1126/science.aai8878)
2. Chazdon RL, Pearcy RW. 1986 Photosynthetic responses to light variation in rain-forest species. 1. Induction under constant and fluctuating light conditions. *Oecologia* **69**, 517–523. (doi:10.1007/bf00410357)
3. Hammond ET, Andrews TJ, Mott KA, Woodrow IE. 1998 Regulation of Rubisco activation in antisense plants of tobacco containing reduced levels of Rubisco activase. *Plant J.* **14**, 101–110. (doi:10.1046/j.1365-313X.1998.00103.x)
4. Soleh MA, Tanaka Y, Nomoto Y, Iwahashi Y, Nakashima K, Fukuda Y, Long SP, Shiraiwa T. 2016 Factors underlying genotypic differences in the induction of photosynthesis in soybean *Glycine max* (L.) Merr. *Plant Cell Environ.* **39**, 685–693. (doi:10.1111/pce.12674)

5. Yamori W, Masumoto C, Fukayama H, Makino A. 2012 Rubisco activase is a key regulator of non-steady-state photosynthesis at any leaf temperature and, to a lesser extent, of steady-state photosynthesis at high temperature. *Plant J.* **71**, 871–880. (doi:10.1111/j.1365-313X.2012.05041.x)
6. FAO. 2016 FAOSTAT. Rome, Italy, Food and Agriculture Organization of the United Nations. url: http://www.fao.org/faostat/en/#home; accessed 12 Dec. 2016.
7. Long SP, Ort DR. 2010 More than taking the heat: crops and global change. *Curr. Opin Plant Biol.* **13**, 241–248. (doi:10.1016/j.pbi.2010.04.008)
8. Ray DK, Mueller ND, West PC, Foley JA. 2013 Yield trends are insufficient to double global crop production by 2050. *PLoS ONE* **8**, e66428. (doi:10.1371/journal.pone.0066428)
9. Ray DK, Ramankutty N, Mueller ND, West PC, Foley JA. 2012 Recent patterns of crop yield growth and stagnation. *Nat. Commun.* **3**, 1293. (doi:10.1038/ncomms2296)
10. Evans LT. 1997 Adapting and improving crops: the endless task. *Phil. Trans. R. Soc. Lond. B* **352**, 901–906. (doi:10.1098/rstb.1997.0069)
11. Zhu XG, Long SP, Ort DR. 2010 Improving photosynthetic efficiency for greater yield. *Annu. Rev. Plant Biol.* **61**, 235–261.
12. Long SP, Marshall-Colon A, Zhu XG. 2015 Meeting the global food demand of the future by engineering crop photosynthesis and yield potential. *Cell* **161**, 56–66. (doi:10.1016/j.cell.2015.03.019)
13. Watanabe N, Evans JR, Chow WS. 1994 Changes in the photosynthetic properties of Australian wheat cultivars over the last century. *Aust. J. Plant Physiol.* **21**, 169–183. (doi:10.1071/PP9940169)
14. Gifford RM, Evans LT. 1981 Photosynthesis, carbon partitioning, and yield. *Annu. Rev. Plant Physiol. Plant Mol. Biol.* **32**, 485–509. (doi:10.1146/annurev.pp.32.060181.002413)
15. Evans LT, Rawson HM. 1970 Photosynthesis and respiration by flag leaf and components of ear during grain development in wheat. *Aust. J. Biol. Sci.* **23**, 245. (doi:10.1071/BI9700245)
16. Sanchez-Bragado R, Elazab A, Zhou BW, Serret MD, Bort J, Nieto-Taladriz MT, Araus JL. 2014 Contribution of the ear and the flag leaf to grain filling in durum wheat inferred from the carbon isotope signature: genotypic and growing conditions effects. *J. Integr. Plant Biol.* **56**, 444–454. (doi:10.1111/jipb.12106)
17. Long SP, Hällgren JE. 1993 Measurement of carbon dioxide assimilation by plants in the field and the laboratory. In *Photosynthesis and productivity in a changing environment: a field and laboratory manual* (eds DO Hall, JMO Scurlock, HR Bolhàr-Nordenkampf, RC Leegood, SP Long) pp. 129–167. London, UK: Chapman & Hall.
18. Long SP, Bernacchi CJ. 2003 Gas exchange measurements, what can they tell us about the underlying limitations to photosynthesis? Procedures and sources of error. *J. Exp. Bot.* **54**, 2393–2401. (doi:10.1093/jxb/erg262)
19. Voncaemmerer S, Farquhar GD. 1981 Some relationships between the biochemistry of photosynthesis and the gas-exchange of leaves. *Planta* **153**, 376–387. (doi:10.1007/BF00384257)
20. Bernacchi CJ, Pimentel C, Long SP. 2003 In vivo temperature response functions of parameters required to model RuBP-limited photosynthesis. *Plant Cell Environ.* **26**, 1419–1430. (doi:10.1046/j.0016-8025.2003.01050.x)
21. Gu LH, Pallardy SG, Tu K, Law BE, Wullschleger SD. 2010 Reliable estimation of biochemical parameters from C-3 leaf photosynthesis-intercellular carbon dioxide response curves. *Plant Cell Environ.* **33**, 1852–1874. (doi:10.1111/j.1365-3040.2010.02192.x)
22. Farquhar GD, Sharkey TD. 1982 Stomatal conductance and photosynthesis. *Annu. Rev. Plant Physiol. Plant Mol. Biol.* **33**, 317–345. (doi:10.1146/annurev.pp.33.060182.001533)
23. Woodrow IE, Mott KA. 1989 Rate limitation of non-steady-state photosynthesis by ribulose-1,5-bisphosphate carboxylase in spinach. *Aust. J. Plant Physiol.* **16**, 487–500.
24. Mott KA, Woodrow IE. 2000 Modelling the role of Rubisco activase in limiting non-steady-state photosynthesis. *J. Exp. Bot.* **51**, 399–406. (doi:10.1093/jexbot/51.suppl_1.399)
25. Zhu XG, Ort DR, Whitmarsh J, Long SP. 2004 The slow reversibility of photosystem II thermal energy dissipation on transfer from high to low light may cause large losses in carbon gain by crop canopies: a theoretical analysis. *J. Exp. Bot.* **55**, 1167–1175. (doi:10.1093/jxb/erh141)
26. Tholen D, Ethier G, Genty B, Pepin S, Zhu XG. 2012 Variable mesophyll conductance revisited: theoretical background and experimental implications. *Plant Cell Environ.* **35**, 2087–2103. (doi:10.1111/j.1365-3040.2012.02538.x)
27. Tholen D, Zhu XG. 2011 The mechanistic basis of internal conductance: a theoretical analysis of mesophyll cell photosynthesis and CO_2 diffusion. *Plant Physiol.* **156**, 90–105. (doi:10.1104/pp.111.172346)
28. Xiao Y, Tholen D, Zhu XG. 2016 The influence of leaf anatomy on the internal light environment and photosynthetic electron transport rate: exploration with a new leaf ray tracing model. *J. Exp. Bot.* **67**, 6021–6035. (doi:10.1093/jxb/erw359)
29. Messinger SM, Buckley TN, Mott KA. 2006 Evidence for involvement of photosynthetic processes in the stomatal response to CO_2. *Plant Physiol.* **140**, 771–778. (doi:10.1104/pp.105.073676)
30. Mott KA, Berg DG, Hunt SM, Peak D. 2014 Is the signal from the mesophyll to the guard cells a vapour-phase ion? *Plant Cell Environ.* **37**, 1184–1191. (doi:10.1111/pce.12226)
31. Sage RF, Cen Y-P, Li M. 2002 The activation state of Rubisco directly limits photosynthesis at low CO_2 and low O_2 partial pressures. *Photosynth. Res.* **71**, 241–250. (doi:10.1023/A:1015510005536)
32. Kaiser E, Kromdijk J, Harbinson J, Heuvelink E, Marcelis LF. M. 2017 Photosynthetic induction and its diffusional, carboxylation and electron transport processes as affected by CO_2 partial pressure, temperature, air humidity and blue irradiance. *Ann. Bot.* **119**, 191–205. (doi:10.1093/aob/mcw226)
33. Kaiser E, Morales A, Harbinson J, Kromdijk J, Heuvelink E, Marcelis LF. M. 2015 Dynamic photosynthesis in different environmental conditions. *J. Exp. Bot.* **66**, 2415–2426. (doi:10.1093/jxb/eru406)
34. Farquhar GD, von Caemmerer S, Berry JA. 1980 A biochemical model of photosynthetic CO_2 assimilation in leaves of C_3 species. *Planta* **149**, 78–90. (doi:10.1007/BF00386231)
35. Carmo-Silva AE, Salvucci ME. 2013 The regulatory properties of Rubisco activase differ among species and affect photosynthetic induction during light transitions. *Plant Physiol.* **161**, 1645–1655. (doi:10.1104/pp.112.213348)